NeuroImage 240 (2021) 118407

Contents lists available at ScienceDirect

NeuroImage

journal homepage: www.elsevier.com/locate/neuroimage

# Spontaneous transient brain states in EEG source space in disorders of consciousness

Yang Bai[a,b,c], Jianghong He[d], Xiaoyu Xia[e], Yong Wang[f], Yi Yang[d], Haibo Di[a], Xiaoli Li[f,*], Ulf Ziemann[b,c,**]

[a] International Vegetative State and Consciousness Science Institute, Hangzhou Normal University, Hangzhou, China
[b] Department of Neurology and Stroke, University of Tübingen, Hoppe-Seyler-Str. 3, Tübingen 72076, Germany
[c] Hertie Institute for Clinical Brain Research, University of Tübingen, Tübingen, Germany
[d] Department of Neurosurgery, Beijing Tiantan Hospital, Capital Medical University, Beijing, China
[e] Department of Neurosurgery, Chinese PLA General Hospital, Beijing, China
[f] State Key Laboratory of Cognitive Neuroscience and Learning, IDG/McGovern Institute for Brain Research, Beijing Normal University, Beijing, China

ARTICLE INFO

*Keywords:*
Transient state
Hidden Markov model
Electroencephalography
Disorder of consciousness

ABSTRACT

Spontaneous transient states were recently identified by functional magnetic resonance imaging and magnetoencephalography in healthy subjects. They organize and coordinate neural activity in brain networks. How spontaneous transient states are altered in abnormal brain conditions is unknown. Here, we conducted a transient state analysis on resting-state electroencephalography (EEG) source space and developed a state transfer analysis to patients with disorders of consciousness (DOC). They uncovered different neural coordination patterns, including spatial power patterns, temporal dynamics, spectral shifts, and connectivity construction varies at potentially very fast (millisecond) time scales, in groups with different consciousness levels: healthy subjects, patients in minimally conscious state (MCS), and patients with vegetative state/unresponsive wakefulness syndrome (VS/UWS). Machine learning based on transient state features reveal high classification accuracy between MCS and VS/UWS. This study developed methodology of transient states analysis on EEG source space and abnormal brain conditions. Findings correlate spontaneous transient states with human consciousness and suggest potential roles of transient states in brain disease assessment.

## 1. Introduction

The human brain can be conceptualized as groups of neural networks that assemble billions of neurons into specific patterns of activity that facilitate global or between-system information transmissions (Power et al., 2010; Power et al., 2011). The organization, interaction, and coordination of the brain networks are thought to provide the physiological basis for any type of higher brain function (Mesulam, 1998; McIntosh, 2000; Bullmore and Sporns, 2009). In response to environmental stimulation, task-specific brain networks are activated and coordinated to transport, process, and represent the information. While the brain is in a resting state, it still builds dynamic configurations spontaneously, to transmit information necessary for vigilance, attention, or upcoming behavior performance (Salvador et al., 2005; Bullmore and Sporns, 2012; Di et al., 2013; Buzsaki, 2006). The network activities could be accompanied by hemodynamic and neurophysiological changes, which can be captured using neuroimaging (e.g., functional magnetic resonance imaging [fMRI]) or electrophysiological (e.g., magnetoencephalography [MEG] and electroencephalography [EEG]) techniques. Understanding the network organization of the brain has been a long-standing challenge in the field of systems neuroscience.

Several methods have been proposed to organize resting-state brain activities into various networks and describe their architectural properties (Rubinov and Sporns, 2010; He and Evans, 2010; Hyafil et al., 2015; Allen et al., 2014). Nevertheless, most of these approaches are limited because they model the brain as single network unit, which ignores the dynamics within modular subnetworks (van den Heuvel and Hulshoff Pol, 2010). To address this problem, a data-driven method based on the Hidden Markov Model (HMM) was proposed to identify how multiregional coordination properties vary over time at potentially very fast (millisecond) time scales (https://github.com/OHBA-analysis/HMM-MAR/wiki). This method infers various discrete brain states that recur at different points in time (Vidaurre et al., 2018a; Quinn et al., 2018). Finally, a series of transient brain networks (transient states) can be identified from brain activities. The transient states show spatially

* Corresponding author.
** Corresponding author at: Department of Neurology and Stroke, University of Tübingen, Hoppe-Seyler-Str. 3, Tübingen 72076, Germany.
*E-mail addresses:* xiaoli@bnu.edu.cn (X. Li), ulf.ziemann@uni-tuebingen.de (U. Ziemann).

https://doi.org/10.1016/j.neuroimage.2021.118407.
Received 11 April 2021; Received in revised form 28 June 2021; Accepted 15 July 2021
Available online 17 July 2021.

distinct patterns of oscillatory power and connectivity, temporal hierarchical organization, correlation/anti-correlation with default mode networks (DMNs), and predicate cognitive traits (Baker et al., 2014; Vidaurre et al., 2018b; Vidaurre et al., 2017). A resting-state MEG study identified 12 spontaneous transient states according to spatial power patterns and phase-coupling features (Vidaurre et al., 2018b). The ongoing cortical activities were presented by the dynamic activation of the underlying transient states. However, because the state inference was based completely on data-driven computation, a fundamental question that remains to be addressed is whether the transient states robustly exist in the human brain. Furthermore, how the analysis of transient states extends our knowledge of brain dynamics and how it will contribute to our understanding of brain diseases still needs to be clarified.

Disorder of consciousness (DOC) encompasses a set of specific conditions—including vegetative state/unresponsive wakefulness syndrome (VS/UWS) (Laureys et al., 2010) and minimally conscious state (MCS) (Giacino et al., 2002)—caused by disruption of the neural activities that sustain human consciousness (i.e., arousal and awareness). Because of complex and multifaceted consciousness impairment mechanisms, abnormal brain networks have been reported frequently in patients with DOC (Bodien et al., 2017), such as DMNs (i.e., anterior medial prefrontal and posterior cingulate cortices) and functional networks outside DMNs, including those involved in processing sensory stimuli and performing higher-order cognitive tasks (i.e., extrinsic networks, such as auditory, visual, sensorimotor, salience, and executive control networks) (Soddu et al., 2012; Vanhaudenhuyse et al., 2010; Wu et al., 2015; Qin et al., 2015). In addition to the spatial construction, temporal dynamics are also an intrinsic property of human spontaneous neural activities (Fox et al., 2005; Deco et al., 2011; Hutchison et al., 2013). Network dynamics can deteriorate despite a globally preserved construction integration; therefore, they should play a crucial role in the evaluation of brain networks (Damaraju et al., 2014; Barttfeld et al., 2015; Breshears et al., 2010). One previous study pointed out that the dynamics of functional connectivity deteriorated with the fading of awareness in patients with DOC (Naro et al., 2018).

Although these studies have revealed relationships between abnormal brain networks and DOC, a more comprehensive understanding of DOC brain networks, which could integrate all the temporal, spatial and dynamic properties of brain activity is warranted. Transient states, estimated by time-delay embedded Hidden Markov model (TDE-HMM) (Vidaurre et al., 2018b), are capable of shedding light on this. Furthermore, transient states from healthy subjects revealed two intrinsic states (anterior and posterior) in resting-state neuronal activity. The investigation of these states in patients with DOC could contribute to an ongoing debate which cortex (prefrontal or parietal cortex) is predominantly responsible for consciousness formation and fading (Koch, 2018; Odegaard et al., 2017; Boly et al., 2017; Koch et al., 2016).

Here, we performed an analysis of transient states in resting-state EEG source space in healthy subjects and patients with DOC, to validate the existence and neurobiological relevance of transient states in the human brain. We investigated the relationship between state-specific features and consciousness levels, and explored the potential neurophysiological implications of transient states in DOC. Transient-state features were used to train a machine learning model to demonstrate their diagnostic utility in discriminating between MCS and VS/UWS, a distinction that is still difficult to make. Thus, we attempted to identify the relationships between spontaneous transient states and human consciousness.

## 2. Materials and methods

### 2.1. Participants

A total 28 healthy participants and 96 patients with DOC were initially recruited into this study. Informed consent to participate in the study was obtained from the healthy subjects and the legal surrogates of the DOC patients. Approval of this study was granted by the Ethics Committee of the PLA Army General Hospital, Beijing, China. For the patients, the inclusion criterion was persistence of a DOC state for at least 1 month after the acute brain insult. The demographic characteristics of the patients are summarized in Table S1 in Supplementary Information. Importantly, the here reported EEG recordings were performed in the first days of hospital treatment, prior to initiation of any medication acting on the central nervous system that could have interfered with interpretation of the EEG findings.

The consciousness diagnosis was based on a behavioral assessment using the Coma Recovery Scale-Revised (CRS-R) (Giacino et al., 2004). Prior to the EEG recording, a trained neurologist conducted a CRS-R assessment at least four times within 1 week, i.e., once per day in the afternoon, for each patient. The CRS-R includes six items that test auditory, visual, motor, oromotor, communication, and arousal function. The scale is both quantitative (scores ranging from 0 to 23, with higher scores indicating a higher level of neurobehavioral function) and qualitative, as it provides subscores that define different states of consciousness (MCS or VS/UWS). The clinical diagnosis was established according to the best consciousness level. The CRS-R was reassessed four times during the week after the EEG recording, to validate the consistency of the clinical diagnosis.

A final cohort of 25 healthy subjects and 62 patients with DOC (MCS, $n = 25$, age (mean $\pm$ 1SD) = $47.5 \pm 14.6$ years, females = 12; VS/UWS, $n = 37$, age = $45.8 \pm 15.9$ years, females = 12) was selected for the analysis. Three healthy subjects and 34 patients were excluded because of an incomplete skull, lack of individual MRI data, artefacts in the EEG signals, or an inconsistent diagnosis at 1 week follow-up (Fig. S1 in Supplementary Information).

### 2.2. MRI scanning and pre-processing

A three-dimensional gradient echo T1 anatomical scan (TR, 1800 ms; TE, 2.5 ms; thickness, 1.0 mm; spacing, 1.0 mm; slices, 176; duration, 4 min 18 s) was obtained and was used to perform the source reconstruction. The MRI pre-processing was performed using a Fieldtrip toolbox (Version 20191014) running in a MATLAB environment (Version 2017b, MathWorks Inc., Natick, USA). The whole volume was resliced onto a $1 \cdot 1 \cdot 1$ $mm^3$ grid aligned with the coordinate axes. The resliced MR images were segmented into three types of tissues: brain, skull, and scalp. Subsequently, an individual cortex mesh was generated from the segmented MR images, and the individual head model was generated from the mesh through the “dipoli” method (Oostendorp and van Oosterom, 1989). Additionally, the individual’s grid was calculated based on the individual MR images and a template grid matrix, which was created on a template MRI in Fieldtrip.

### 2.3. EEG recording and processing

The EEG recording setup was consistent across all participants. The EEG data were acquired using a 64-channel EEG recorder (BrainAmp 64 MRplus, BrainProducts) equipped with sintered Ag/AgCl pin electrodes. We set a band-pass filter at DC to 1000 Hz in the recorder. The EEG signals were digitized at a sampling rate of 2.5 kHz. The skin/electrode impedance was maintained below 5 kΩ. Each recording lasted 10 min. Healthy subjects were placed in a lying position on a bed and maintained an arousal state (eyes open) during the recordings. For the patients, a CRS-R arousal facilitation protocol was performed immediately before the EEG recording to keep them aroused during EEG recording. If a patient closed eyes for more than several seconds, the EEG recording was terminated, the data discarded, and the CRS-R arousal facilitation protocol and EEG recording repeated. Participants received no nutrition within 30 min before and during the EEG recordings.

An offline pre-processing was performed using EEGLAB 12.0.2.5b running in the MATLAB environment. First, the EEG data were band-pass filtered (1-40 Hz) and downsampled to 250 Hz. Then, the data

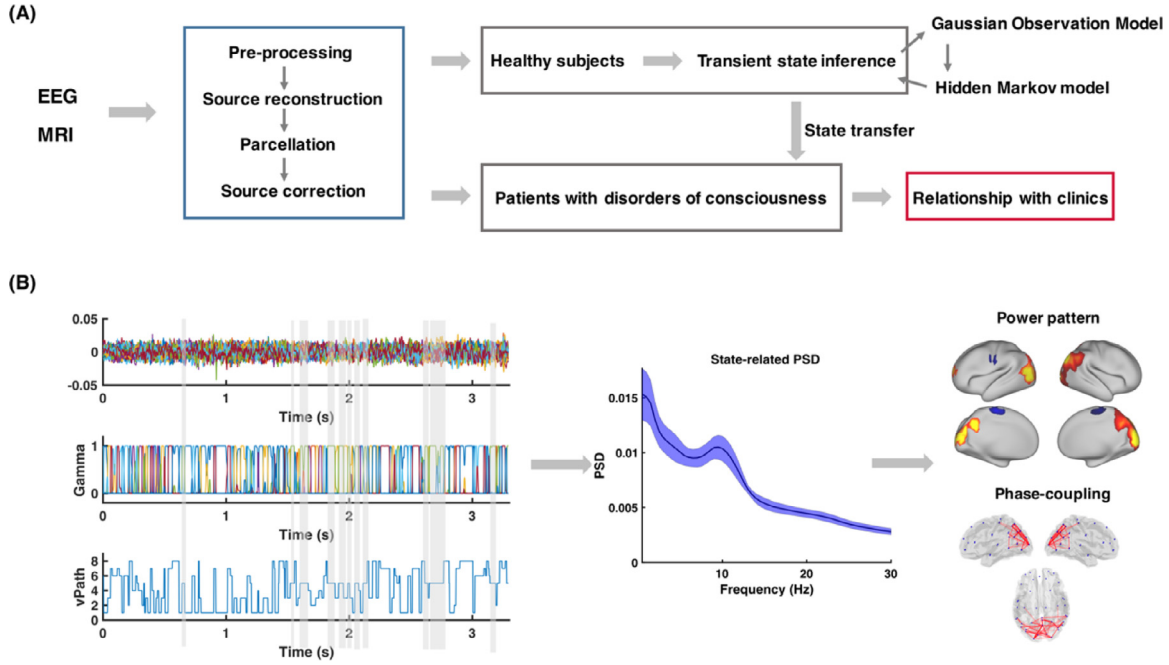


**Fig. 1.** Schematic pipeline of the transient state analysis. (*A*) Transient state analysis in healthy subjects and patients with disorders of consciousness. The state parameters were extracted from healthy subjects by a method that combined the Gaussian observation model and the Hidden Markov Model on EEG source space. The parameters from healthy subjects were used to infer the state activities in each patient. (*B*) Illustration of the state segmentation and the power/connectivity analysis. The state-specific power spectral density (PSD) was calculated from the identified state epochs (the gray bars show the identified epochs of one state). Spatial power and connectivity were measured based on the PSD of each state (in this case the visual transient state is shown as an example).

were segmented into epochs (8 s each, without overlap). Bad channels and epochs were detected and removed by combining Wiener estimation (Mutanen et al., 2018) with visual spectrum judgment. A "fastica" algorithm-based independent components analysis (Hyvarinen and Oja, 2000) was conducted on the retained epochs. Topography, weights in the epochs, and the spectrum were used to detect and remove eye blinking/movement components. A butterfly plot of the power spectrum was generated to check visually whether bad channels, epochs, or distinct artefacts remained in the data; if so, the above process was repeated. Finally, the bad channels were interpolated using a spherical method.

The electrodes were aligned to the individual head model based on manual matching and automatic projection. The individual lead field matrix was calculated based on the aligned electrodes, individual grid, and head model. The source reconstruction was performed using a linearly constrained minimum variance beamforming (Hillebrand and Barnes, 2005). The whole source space was parcellated into 42 dipoles, and source activities were projected into these 42 dipoles based on a weighted mask and principle component analysis. The dipoles were obtained from the Human Connectome Project (Colclough et al., 2016; Vidaurre et al., 2018b). Spatial leakage and the arbitrary dipole polarity were then resolved according to the methods proposed in reference (Vidaurre et al., 2018b) (Fig. 1*A*).

### 2.4. Time-delay embedded Hidden Markov Model (TDE-HMM)

In this work, the hidden transient states were inferred on the group-concatenated source activity from the healthy subjects using the HMM-MAR toolbox (https://github.com/OHBA-analysis/HMM-MAR). This approach assumes that the EEG activities from the healthy subjects are driven by several transient states, which were described using a multivariate normal distribution. The data were segmented by state labels according to probabilistic observation models. Different probabilistic distributions were used to model the properties of the transient states. The model selection depends on an assumption concerning the types of information driving the data. The current work referred to references (Baker et al., 2014; Vidaurre et al., 2018b) and used the time-delay embedded Gaussian distribution to focus on power patterns and phase coupling in the resting-state EEG (Fig. 1*B*).

The transient states were inferred using variational Bayesian inference on the HMM. According to the transient state assumption, only one state is active at each time point. The expression of the current state depends on the current observation (probability distribution described by the observation model) and the past state (transition probability within states). The number of states (K) in the data, which should be specified before the model inference, depends on the prior knowledge and hypotheses. The details of parameter selection for the determination of the number of states in this work is provided in the Supplementary Information. Further details about the inference process on the model can be found in reference (Vidaurre et al., 2018b).

Similar to a previous MEG study (Vidaurre et al., 2018b), an "embedding" time window (60 ms) was used to build up the states' description, including not only the spatial activation pattern, but also the temporal oscillation; i.e., at each time point, t, the autocovariance matrix (i.e., the total number of points × the total number of regions by the total number of points × the total number of regions; 15 × 42 by 15 × 42 in this work), which was measured within the 30 ms preceding and following time point t across the whole brain region, was used to infer the hidden transient state for time point t. However, to simplify the computation and concentrate on common information, the states' distributions were described through principal component analysis (PCA) decomposition (84 PCs from a total of 630 PCs, explaining an average of 66.5% of the variance). Additionally, based on the discontinuous nature of the epochs in time, the state inference should end at the end of the epoch and should start at the beginning of each epoch.

### 2.5. State transfer

To render the states comparable between different groups, the present study included a states transfer analysis from healthy subjects

to patients with MCS and VS/UWS (Fig. 1*A*). Specifically, after inferring the states of the healthy subjects, the transient states could be described by Gaussian observation model bases using different parameters (i.e., a covariance matrix on the PCA space [84 × 84 in this work] and a scaling gain) in the same model framework. These observation models were driven by the common information from EEG of healthy subjects and captured structural patterns of oscillatory power and covariance within multi-regions in time-delay embedded PCA space. Based on the observation model of such states, the probability distribution of each real observation (an embedded covariance matrix corresponding to a time point centered at a 60 ms time window) of the states could be estimated in respect to the observation model family by likelihood measures (see details in Supplementary Information). Then, for each patient, an HMM process was used to explore the hidden state at each time point. Therefore, the source activities of the patients could be segmented into the specific time windows of different states according to their probabilistic belonging distribution and their history of state expression.

### 2.6. Specific features of the transient states

Three types of state-specific features were measured in this work: power spectrum density (PSD), connectivity, and temporal features. PSD and connectivity were extracted from the states' segmented source activities using a multitaper and coherence approach. PSD indicates state-wise activation power patterns and coherence measures regarding the phase-coupling relationship within different brain regions. To visualize the state-wise power pattern and connectivity feature, nonparametric statistical testing (a permutation test) was used to indicate the significance of the state-specific power and connectivity (Vidaurre et al., 2018b).

Additionally, to investigate the state-specific differences between patients with purposeful or non-purposeful behavioral responses, betweenness values based on the state network were measured (for details, see Supplementary Information). The betweenness evaluates the hub role of nodes in the whole state network. Furthermore, the sequence of transient states over time of each participant was described using three types of temporal features: fractional occupancy, dwell time, and interval time. The fractional occupancy refers to the total time spent by each participant in each state. The dwell time and interval time refer to the lasting time of each state's expression and the interval between two visits of each state, respectively. Finally, state transition was used to present the states' temporal relationship, as it measures the probability of adjacent combinations (from one state to another).

### 2.7. Machine learning

A machine learning structure was designed to evaluate the state-wise features in classifying MCS and VS/UWS (Fig. S10 in Supplementary Information). To avoid overfitting caused by the small number of samples (n = 62), a feature selection strategy (based on bootstrap sampling) combined with nest structured machine learning was used to construct the binary classification model. The classification model was built through a partial least squares (PLS) regression combined with a linear discriminant analysis (LDA) (Li et al., 2018). A double leave-one-out cross-validation and competitive adaptive reweighted sampling (CARS) method based on parameter optimization was used to achieve good generalization performance. The details are provided in the Supplementary Information. CARS is a sampling-based strategy for key-feature selection performed via the optimization of model performance.

### 2.8. Data availability

The MATLAB scripts—including the EEG and MRI pre-processing pipeline, source construction and parcellation, transient state inference and transfer, and machine learning—are available at the https://github.com/BYJW/EEG-Transient-State. Related toolboxes can be accessed at https://github.com/OHBA-analysis and http://libpls.net/. Original EEG datasets including healthy subjects and patients with DOC can be accessed with *link* (https://drive.google.com/drive/folders/1CFx1Q3RqZq5Vzig2tSUA1pFyloxBBuoB?usp=sharing). Because of the privacy regulations of the collaborating hospital, the individual MR images can only be accessible by contacting Dr. Yi Yang (one of the authors, affiliation see above) with research application.

## 3. Results

### 3.1. Four key transient states in the EEG source space from healthy subjects

Inferring transient states using TDE-HMM was a completely data-driven process. Depending on the number of states (K), the inference finally found the state expression sequence underlying the observed source activities. The K value determined the cluster of Gaussian observation model bases, which used different parameters to describe the state properties. The K value should be given before the model training, according to prior knowledge or research hypotheses. In the current study, according to previous MEG results (Vidaurre et al., 2018b), we initially hypothesized that the resting state of the EEG source activities would be a mixture of 12 underlying state expressions. Then, the state expression in each subject was checked to determine the final number of states, which should be commonly shared among most of the subjects (for more details, see Supplementary Information). However, even when inferred using different numbers of states (K = 8, 10, and 12), four key states were always identified from the EEG source activities (Figs S2 and S3 in Supplementary Information). They were named according to their specific spatial active patterns and phase coupling: anterior, posterior, sensorimotor, and visual. These key transient states from the EEG source space presented similar features to the four main states identified from the previous MEG study (Vidaurre et al., 2018b): anterior high-order cognitive, posterior high-order cognitive, sensorimotor, and visual states. The four key states had different spectral properties, spatial power patterns, and functional connectivities. The anterior state was characterized by a significantly higher anterior delta power (t-test with FDR correction) compared to the anterior delta power during the expression of any of the other key states (Fig. 2*A, B*). It also showed significant connectivity within the anterior regions (permutation tests, $P < 0.01$) (Fig. 2*C*). The posterior state was characterized by a strong alpha power and had significant connectivity within the parietal regions. Similarly, the sensorimotor and visual states showed sensorimotor- and visual-specific activities in the alpha band and alpha-low beta band, respectively (Fig. 2).

### 3.2. Four key transient states in patients with DOC

To allow the comparison of the patients' states with those of the healthy subjects, we performed a state transfer analysis on the patients with DOC. The Gaussian observation model bases from the healthy subjects were used to segment the EEG source activities from the patients. Therefore, state segmentation for all of the participants was based on the same substrates. After the transfer analysis, the spectral features were calculated from the segmented EEG source activities. The results showed that, although there were slight distortions in the patients compared with the healthy subjects, the identified four key transient states still preserved their specific spatial power patterns (Fig. 3) similar to the states in healthy subjects. The patients with MCS showed more extensive significant connectivity than did those with VS/UWS in all states (Fig. 3).

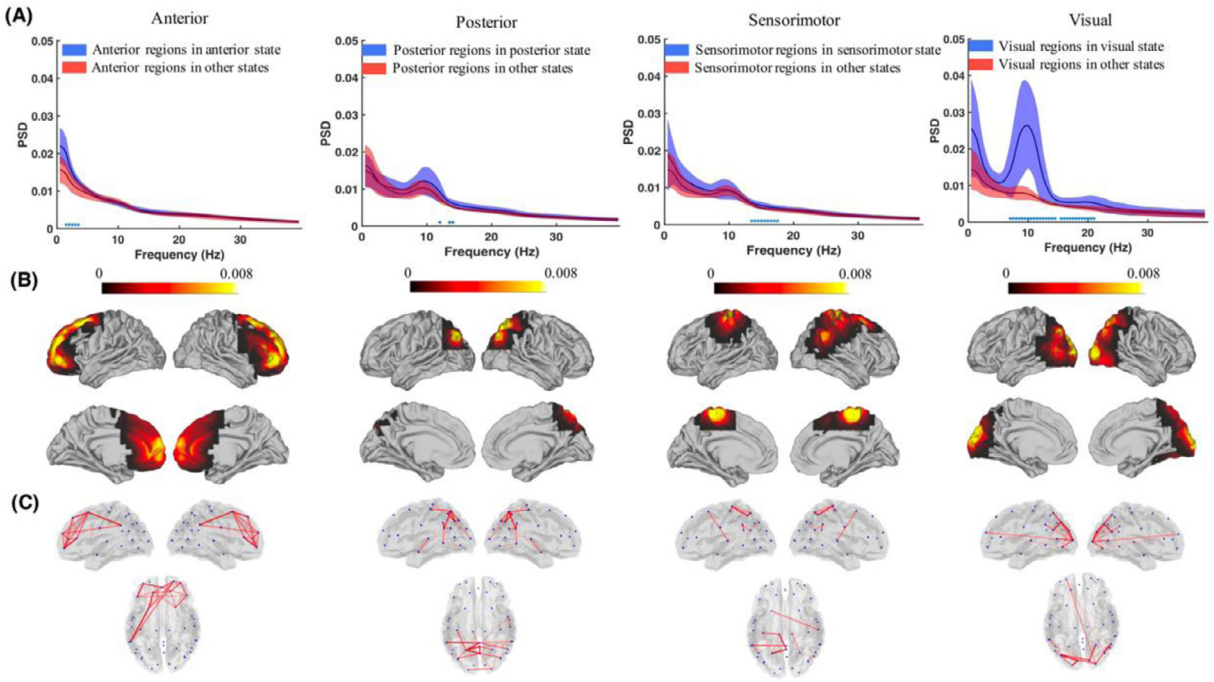


**Fig. 2.** Power and connectivity properties of the key transient states (anterior, posterior, sensorimotor, and visual) identified in the EEG source space from healthy subjects. (*A*) Power spectral density (PSD) in the state-specific brain regions (means ± 1SD) during the investigated state (blue) and during the other key states (red). The asterisks under the curves indicate statistical significance between the investigated state and the other key states (t-tests with FDR correction, $P < 0.05$). (*B*) Significantly higher power of the investigated state compared with all other key states (permutation tests, level of statistical significance, $P < 0.01$, color bars indicate activation power). (*C*) Significantly stronger functional connectivity of the investigated state compared with all other key states (indicated by red lines, permutation tests, level of statistical significance, $P < 0.01$) (For interpretation of the references to color in this figure legend, the reader is referred to the web version of this article.).

### *3.3. Impaired transient state dynamics and connectivity in patients with DOC*

Three temporal features were obtained based on the expression sequence of the transient states: fractional occupancy (Fig. 4*C*), dwell time, and interval time (Fig. S8 in Supplementary Information). All three features showed significant differences between healthy subjects and patients with MCS and VS/UWS. Compared with the healthy subjects, patients with DOC spent more time in the anterior state ($P < 0.001$, two-sample *t*-test) and less time in the posterior state ($P < 0.001$) (Fig. 4*C*). For the patients with DOC, the temporal features of state expression were also different between patients with MCS and those with VS/UWS. Statistical analysis was performed with paired two-tailed *t*-tests FDR-corrected for multiple comparisons (4 key transient states x 3 groups). Fractional occupancy of the anterior state was greater in VS/UWS than MCS ($P = 0.003$), while fractional occupancy of the sensorimotor ($P = 0.003$), and visual ($P = 0.001$) states was lower in VS/UWS than in MCS, or showed a strong trend towards this difference in the posterior state ($P = 0.005$). The higher fractional occupancy of the anterior state observed in VS/UWS vs. MCS was mainly caused by the difference in dwell time (mean ± 1SD): 121.4 ± 4.1 ms in VS/UWS vs. 72.7 ± 3.8 ms in MCS (Fig. S8 in Supplementary Information). Conversely, the lower fractional occupancy of the posterior state in VS/UWS compared to MCS was mainly caused by the smaller number of appearances, as there was a longer interval time. State transitions can also be measured from the state expression sequence. As shown in Fig. 4*A*, the transition both in and out of the posterior state was significantly suppressed (two-sample *t*-tests with $P < 0.05$ after FDR correction) in patients with DOC compared with healthy subjects. In contrast, the transition from the sensory states (sensorimotor and visual states) to the anterior state was significantly increased. Moreover, patients with VS/UWS showed a decreased transition between the sensory and posterior states compared to patients with MCS (Fig. 4*B*).

In addition, we investigated two DMN nodes (medial prefrontal cortex [mPFC] and posterior cingulate cortex [PCC]) in the anterior and posterior states, which were considered closely correlated with DMN (Raichle et al., 2001; Fransson and Marrelec, 2008). Fig. 5 shows the power in the mPFC and PCC and the coherence between them in the anterior and posterior states. Coherence in the alpha band between the mPFC and PCC was found to be disrupted in MCS and VS/UWS compared to healthy subjects in the anterior state (two-sample *t*-test, $P < 0.05$ with FDR correction).

### *3.4. Sensory states were correlated with purposeful behavior in patients with MCS*

As behavioral consciousness assessments (e.g., CRS-R) are focused mainly on external awareness, the above reported differences of sensory state features (sensorimotor, visual) between healthy subjects, patients with MCS, and patients with VS/UWS motivated us to investigate the relationship between sensory state expression and the corresponding behavior. According to the 1-week motor/visual behavioral assessments using the relevant CRS-R subscales, the DOC patients were divided into different groups based on their behavioral responses. In the motor assessment, the patients who could locate the noxious stimulation, the object manipulation, or were even capable of higher purposeful motor function (best motor score higher than 2, supplementary table S1) were classified into the purposeful motor group (MCS-M). In the visual assessment, the patients who showed fixation, visual pursuit, or higher visual function (best visual score higher than 1, supplementary table S1) were classified into the purposeful visual group (MCS-V). None of the patients with VS/UWS displayed purposeful behaviors, while some of the patients with MCS exhibited purposeful motor and/or visual behaviors (Figs. 6*A* and 7*A*; for more details, see Supplementary Information).

Among the patients with MCS, 13/25 individuals showed only passive behavioral responses (MCS-NM) in the motor assessment (Fig. 6*A*).

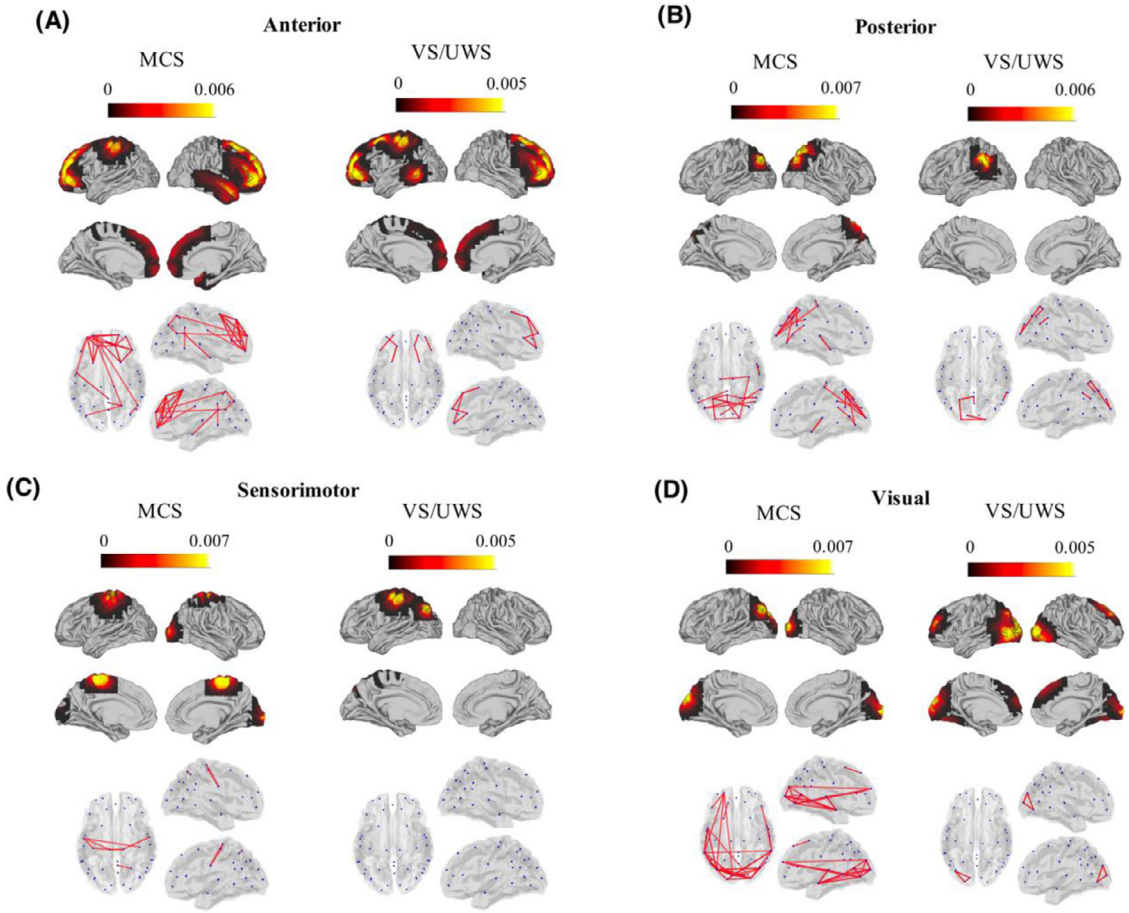


**Fig. 3.** The four key transient states (*A–D*: anterior, posterior, sensorimotor, and visual) identified in patients with disorders of consciousness. The spatial active maps show significantly higher power values of the investigated state compared to other key states (permutation tests, level of statistical significance, $P < 0.01$; color bars indicate activation power). The red lines indicate significantly higher functional connectivity in the investigated state compared to all other key states (permutation tests, level of statistical significance, $P < 0.01$). Note the reduced level of state-dependent connectivity expression in patients with vegetative state/unresponsive wakefulness syndrome (VS/UWS) compared to patients with minimally conscious state (MCS) (For interpretation of the references to color in this figure legend, the reader is referred to the web version of this article.).

Specific to the sensorimotor state expression, the MCS-M group showed significant enhancement of power in the beta band in the left sensorimotor region compared with the MCS-NM group (Kolmogorov-Smirnov test with FDR correction, $P < 0.05$, Fig. 6*B*). The beta enhancement did not appear at the sensorimotor regions during expression of any of the other key transient states (Fig. S9A in Supplementary Information). Additionally, the MCS-M group exhibited stronger connectivity (i.e., higher coherence values) in the beta frequency range with the right sensorimotor region than the MCS-NM group (Kolmogorov-Smirnov test with FDR correction, $P < 0.05$; Fig. 6*C*). The network analysis revealed that one left and three right sensorimotor regions showed significantly higher betweenness values in MCS-M than MCS-NM (Fig. 6D), which suggests that these sensorimotor regions play a stronger hub role in the sensorimotor state expression in MCS-M compared to MCS-NM.

6/25 patients with MCS showed no purposeful visual behaviors (MCS-NV) (Fig. 7*A*). The comparison of the PSD between MCS-V and MCS-NV in visual state expression revealed a significant difference in the bilateral visual regions. Patients with MCS-V had higher alpha-low beta (8.5–19.5 Hz) power in the visual region than did the MCS-NV group (Kolmogorov-Smirnov tests with FDR correction, $P < 0.05$) (Fig. 7*B*) during the visual state expression. There was no difference of the PSD at the visual regions during expression of any of the other key states (Fig. S9*B* in Supplementary Information). Moreover, the bilateral visual regions showed higher coherence (Fig. 7*C*) and higher betweenness (Fig. 7*D*) in patients with MCS-V vs. those with MCS-NV in the alpha-low beta band.

### 3.5. State features that classified MCS and VS/UWS

The transient states showed differences between MCS and VS/UWS. We detected many state-specific features (including PSD, state dynamics, and connectivity) that were significantly correlated with the patients' CRS-R scores. According to the CRS-R-based clinical diagnosis, we trained a machine learning model using the state-specific features to classify MCS and VS/UWS. The machine learning model used the coupling of partial least squares regression (PLSR) and linear discriminant analysis (LDA) to establish the linear projection between the transient state features and consciousness states (details provided in Supplementary Information). The nest structure, combined with two feature selection strategies, was used to train the classification model.

A total of 84 transient state features were identified for the machine learning classification. They included three types of temporal features for each key transient state (3 features × 4 states, 12 in total), and 36 power features and 36 connectivity features at the states' specific frequency bands and specific nodes (for details, see Supplementary Information). Several of them showed significant correlations with the patients' total CRS-R scores (Fig. 8*A*). We conducted statistical testing (two-sample *t*-tests, $P < 0.05$) and competitive adaptive reweighted sampling (CARS) method on 1000 bootstrap sampling sets with all features (see Supplementary Information). This highlighted several features (with threshold value Tr = 264), including seven power features (four anterior-state-specific nodes and three posterior-state-

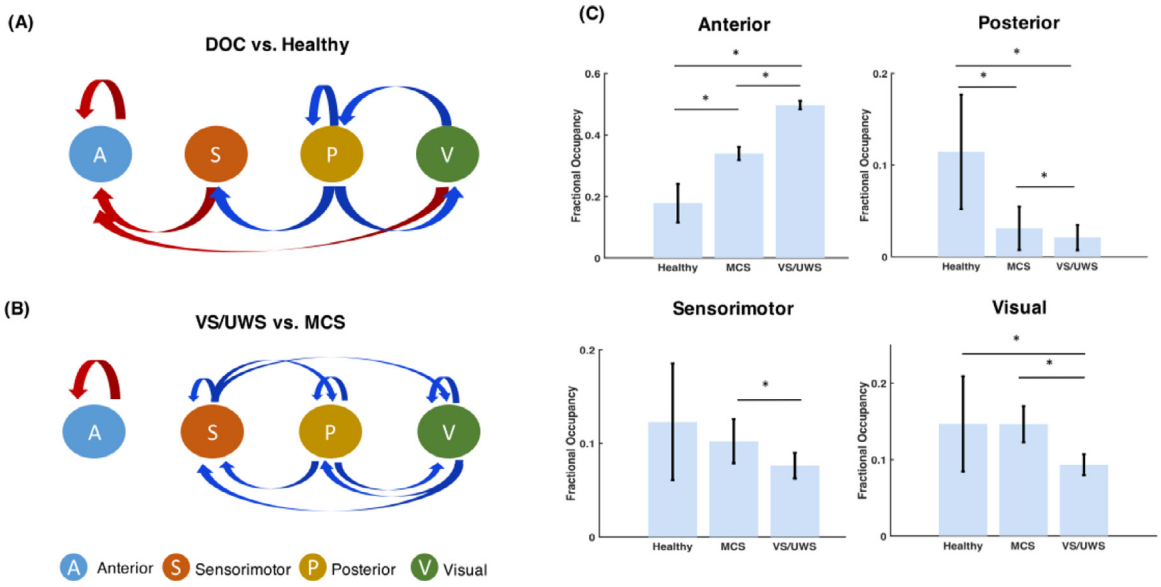


**Fig. 4.** The transition (from state to state) and fractional occupancy of the four key transient states (anterior, posterior, sensorimotor, and visual) identified in healthy subjects and patients with disorders of consciousness (DOC). (*A*) State transition difference between patients with DOC and healthy subjects. (*B*) State transition difference between patients with minimally conscious state (MCS) and those with vegetative state/unresponsive wakefulness syndrome (VS/UWS). The red arrows indicate a significant increase in transition, while the blue arrows indicate a significant decrease in transition. Significance was tested by two-sample *t*-tests with $P < 0.05$ after FDR correction. (*C*) The fractional occupancy (means ± 1SD) was significantly different between healthy subjects and patients with MCS and VS/UWS. * indicates significance after FDR correction. Fig. S8 (Supplementary Information) shows the dwell time and interval time data (For interpretation of the references to color in this figure legend, the reader is referred to the web version of this article.).

specific nodes, Fig. 8*B*) and two connectivity features (visual-state-specific states, Fig. 8*B*), in distinguishing MCS and VS/UWS patients.

Subsequently, the feature selection strategy was applied in each inner layer of machine training using the combination of statistical tests (two-sample *t*-tests, $P < 0.05$) and CARS method on 50 bootstrap sampling sets (for details, see Supplementary Information) to reduce the number of features in each fold of model learning. Firstly, we tested the machine learning on 84 features (including power spectral density of 42 nodes and magnitude-squared coherence strength of 42 nodes) from all time series, disregarding transient states. A total accuracy of 74% was achieved in classifying MCS vs. VS/UWS (for details, see Fig. S11 and Supplementary Information). Afterwards, the 84 transient state features were given into the same machine learning structure. The PLSR-LDA model generated prediction scores for each patient (Fig. 8*C*). The model reached 86% accuracy in detecting patients with VS/UWS and 76% accuracy in detecting patients with MCS. The total classification accuracy reached 82%. The area under the receiver operating characteristic curve was 0.91. Furthermore, the prediction scores showed a close positive correlation ($r = 0.64$, $P < 0.001$) with the patients' CRS-R total scores (Fig. 8*D*). The coefficient of determination was 0.41, with a root mean squared error of 0.62.

## 4. Discussion

The existing literature reports a series of transient states in fMRI and MEG studies (Baker et al., 2014; Vidaurre et al., 2016; Vidaurre et al., 2018a). The transient states, which could be considered as brain subnetworks, showed specific temporal dynamics, spatial activation, and correlation with different types of information processing. In response to environmental stimulation, specific transient states in the brain are activated to process the task-related information (Vidaurre et al., 2018a; Quinn et al., 2018). When the brain is in resting state, several transient states, including four key states—anterior, posterior, sensorimotor, and visual—, were identified with MEG (Vidaurre et al., 2018b). By using TDE-HMM, the current study explored the transient states using resting-state EEG. The results showed that the four key states, which identify specific spatial activation patterns and phase coupling, also exist in the EEG source space. Using the Gaussian observation model bases obtained from healthy subjects, we performed a transfer analysis in the EEG space of patients with DOC. The features of the transient states showed significant differences between the different consciousness groups (healthy subjects, MCS, VS/UWS), indicating a physiologically relevant correlation between the spontaneous transient states and human consciousness.

Although the four key transient states of the healthy subjects were found in patients with DOC, with similar power patterns and phase-coupling features, the dynamics of the expression of the transient states was altered. For example, fractional occupancy was significantly increased for the anterior state and decreased for the posterior state, and state switching was significantly suppressed in the DOC patients, which indicates a decrease in brain network dynamics. This method differs from conventional dynamic connectivity research, which investigates changes in network construction. However, across methodologies, the findings consistently demonstrate a network dynamics decrease in individuals with consciousness disorders (Naro et al., 2018).

The subnetworks identified by the anterior and posterior states exhibited a strong correlation with DMN (Vidaurre et al., 2018b). Although a debate remains regarding the cognitive functions of the DMN, PET and fMRI studies have shown that activity in DMN is closely correlated with a patient's level of conscious awareness (Soddu et al., 2012; Vanhaudenhuyse et al., 2010; Wu et al., 2015; Rosazza et al., 2016), which was considered as an important index for distinguishing between MCS and VS/UWS (Demertzi et al., 2014; Demertzi et al., 2015). We showed that functional connectivity in DOC patients between the mPFC and the PCC, which are critical frontal and parietal nodes in the DMN, was broken down in the alpha band during presence of the anterior state. There is now increasing evidence that the disconnection of frontoparietal connectivity within the DMN is linked to a fading of consciousness (Lee et al., 2009; Boly et al., 2012; Thul et al., 2016). The current findings support the consistent conclusion of previous studies: DMN connectivity is disrupted in patients with DOC (Huang et al., 2014; Vanhaudenhuyse et al., 2010).

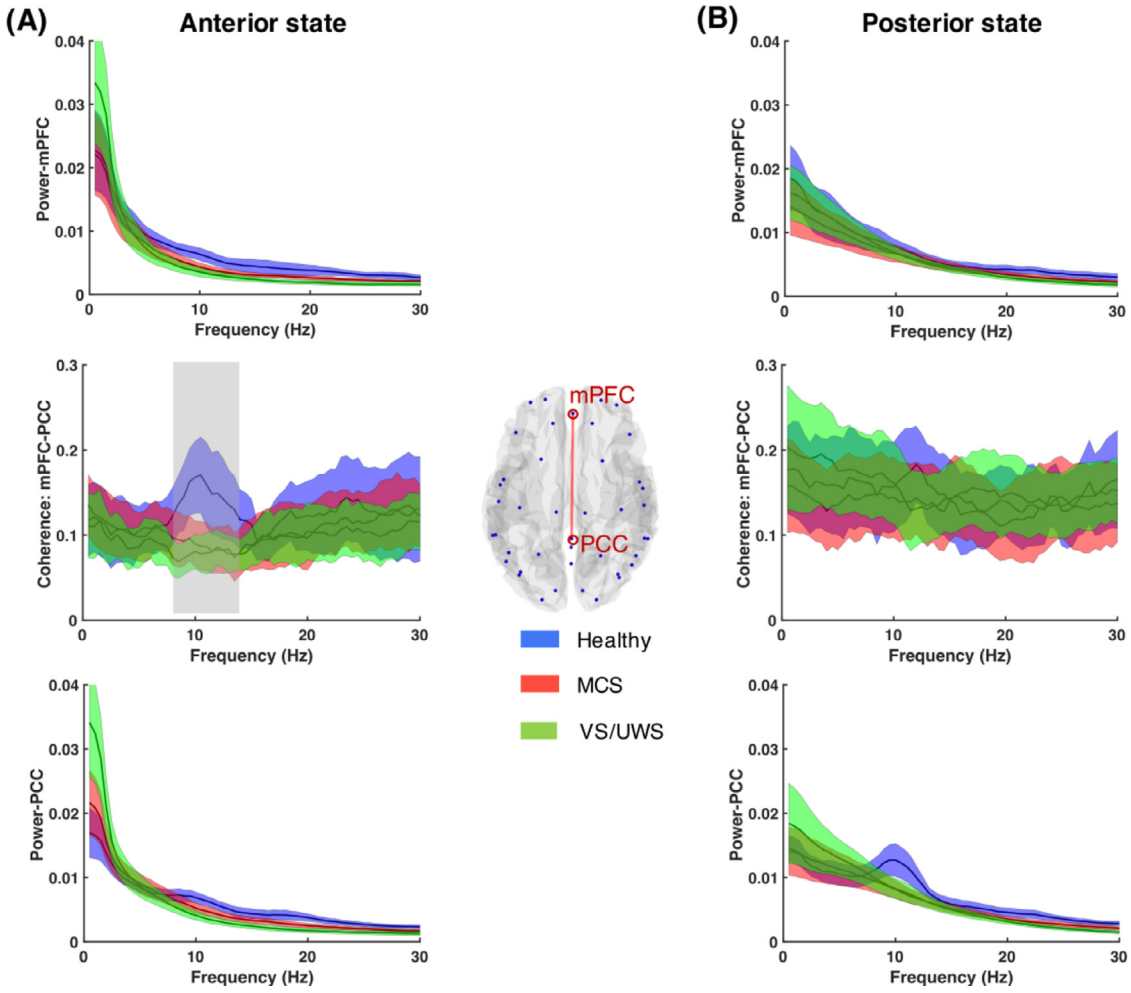


**Fig. 5.** Power and coherence (means ± 1SD) of the medial prefrontal cortex (mPFC) and posterior cingulate cortex (PCC) in the anterior (*A*) and posterior (*B*) key transient states. The panels at the top and bottom show the spectral power of the mPFC and PCC, respectively. The panels in the middle show the coherence between the mPFC and PCC as a function of the frequency. Blue, healthy subjects; red, patients with minimally conscious state (MCS); and green, patients with vegetative state/unresponsive wakefulness syndrome (VS/UWS). The gray area indicates a significant difference (two-sample *t*-test with FDR correction, $P < 0.05$) between the healthy subjects and patients with MCS and VS/UWS in the anterior state (For interpretation of the references to color in this figure legend, the reader is referred to the web version of this article.).

In recent years, many consciousness studies have debated the role of the prefrontal cortex and posterior cortex in the process of consciousness formation (Koch, 2018; Odegaard et al., 2017; Boly et al., 2017; Koch et al., 2016). However, there is increasing evidence that the posterior cortex may be a more decisive brain region for consciousness (Koch, 2018; Boly et al., 2017; Koch et al., 2016; Selimbeyoglu and Parvizi, 2010), as consciousness could be retained even after the removal of most of the prefrontal cortex of patients (Boly et al., 2017; Koch et al., 2016). The results of the current study also provided evidence that highlighted a more critical position of the posterior state in consciousness: a decrease of the posterior state and an increase of the anterior state expression accompanied a decrease in consciousness. In fact, the DOC network was trapped in the anterior "island" (increased fractional occupancy of the anterior state), losing dynamics (decreased state transition) and information interaction (decreased connectivity with other brain regions, Fig. 6*A*). Such low-dynamic and disconnected networks go against the foundation of human consciousness (Ferrarelli et al., 2010; Tononi et al., 2016) and may be one of the pathophysiological mechanisms of DOC (Casali et al., 2013).

In addition to "intrinsic" networks (anterior and posterior states), we identified an additional two sensory networks: the sensorimotor and visual states. These states are linked to cognitive processes of the external sensory input and are considered as composing the "extrinsic" network system (Damoiseaux et al., 2006). Our results demonstrated that the sensorimotor and visual networks are also correlated with consciousness levels, highlighting their contribution to consciousness awareness (Demertzi et al., 2015; Martinez et al., 2020; Yao et al., 2015). In patients with DOC, the connection strength, fractional occupancy, and the transitions of sensory networks were decreased. Consistent with a previous study (Demertzi et al., 2015), the activation of the sensory network showed a positive correlation with patients' CRS-R scores. Patients with MCS showed significantly higher fractional occupancy and shorter interval times of the sensory states than patients with VS/UWS. At the same consciousness level, compared with patients who only had passive behavioral responses, the patients who retained the ability to perform purposeful behaviors exhibited stronger power and connectivity in the corresponding sensory states. This finding offers new evidence supporting the idea that consciousness related to specific sensory input could be predicted by the activation pattern of the corresponding sensory cortex (Andersen et al., 2016; Boly et al., 2017). However, other factors may limit the patients' conscious behaviors, which could possibly produce a bias in the results. For example, some patients exhibit a type of "cognitive motor dissociation" with an extremely limited ability to move but with preservation of higher-level cognition in the form of reliable

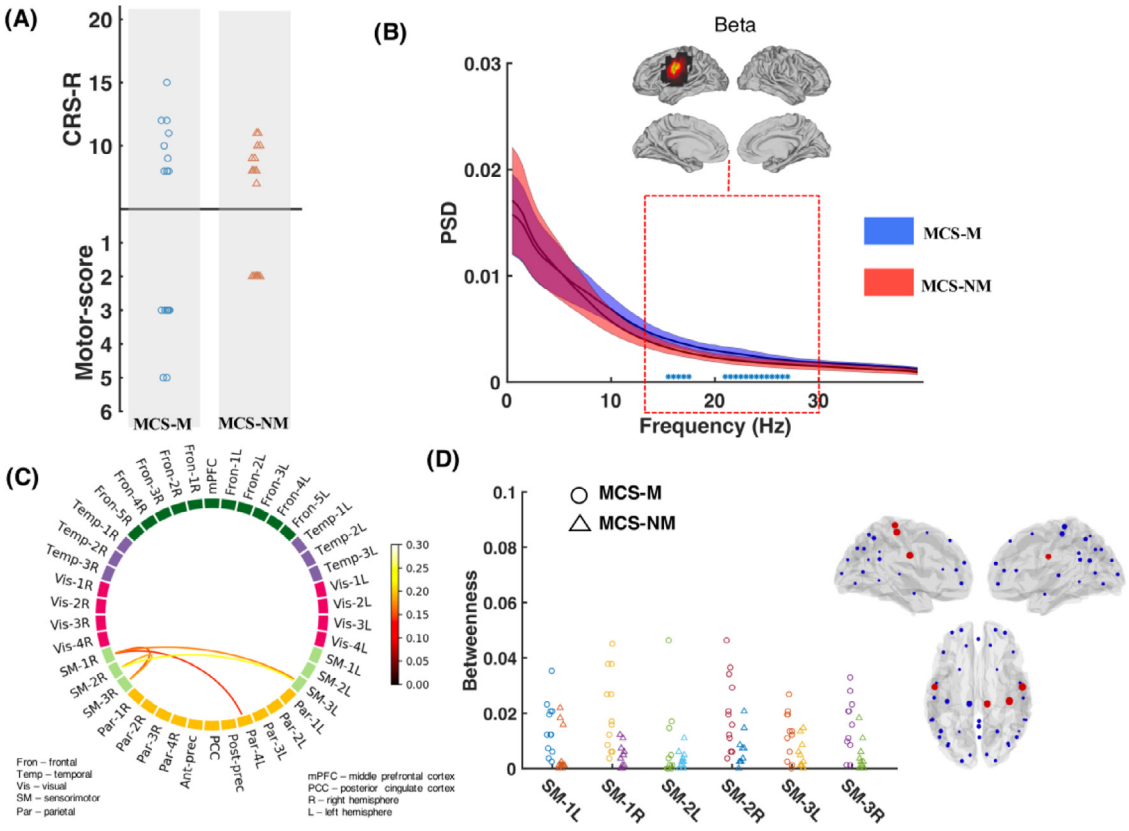


**Fig. 6.** Sensorimotor transient state in patients with a minimally conscious state (MCS). (A) Patients were classified into two groups according to the CRS-R motor behavioral assessment: presence of purposeful motor responses (MCS-M, CRS-R motor score >2) or not (MCS-NM). (B) The PSD – frequency plot (mean ± 1SD; blue: MCS-M, red: MCS-NM) shows the frequency bins with group difference (* Kolmogorov–Smirnov tests with FDR correction, P<0.05) at the motor regions during sensorimotor state expression. Patients with MCS-M exhibited higher power in the beta band compared with MCS-NM in the left sensorimotor regions (spatial plots) during sensorimotor state expression. (C) Lines in the connectivity plot representing the source space with 42 parcellations indicate significantly stronger connectivity (i.e., higher coherence values) in the beta band of MCS-M vs. MCS-NM during the sensorimotor state expression. The color of the lines represents connectivity strength, as given in the color bar. (D) Hub values (betweenness) of the sensorimotor regions in MCS-M and MCS-NM. The sensorimotor regions played a significant hub role during sensorimotor state expression in MCS-M. The dot sizes represent betweenness values, with the red ones indicating significantly higher hub values of MCS-M compared to MCS-NM (For interpretation of the references to color in this figure legend, the reader is referred to the web version of this article.).

command following, as detected using fMRI, EEG, or other noninvasive measures of brain activity (Schiff, 2015). The lack of observed purposeful behaviors does not imply the absence of functional sensory states or networks. The current study highlighted the roles of transient sensory network states in consciousness.

All four key transient states inferred from the HMM showed specific spectral features. The anterior state was dominated by low-frequency activity (delta band), while the other states had relatively higher-frequency activities (alpha and beta bands). The delta and alpha bands are the most commonly identified frequency bands to distinguish patients with VS/UWS, MCS and healthy subjects. The enhanced delta and suppressed alpha activities have been used as markers of a low consciousness level (Rossi Sebastiano et al., 2015). The delta power of patients with VS/UWS is higher and the alpha power lower than in patients with MCS (Piarulli et al., 2016; Naro et al., 2016). Regarding functional connectivity, patients with lower consciousness appeared to have a greater disruption of connectivity in the alpha band than patients with better consciousness (Lehembre et al., 2012). The findings of our study are consistent with those of previous studies. The increase in the fractional occupancy of anterior states in DOC represented a domination of low-frequency (delta) activity in the resting-state EEG. The decrease in posterior and visual state expression was consistent with the decrease in alpha activities and connectivity. In addition to the spectrum power shift, our study also identified a spatial shift: from alpha at the posterior cortex to delta at the anterior cortex. Such temporal and spatial shifts were also partly revealed in microstate analyses. A lower probability of the occurrence of an alpha-rhythmic microstate was found in patients with DOC compared to healthy subjects (Fingelkurts et al., 2012). Thus, the lack of awareness in patients with DOC might be related with the domination of the low-frequency state and the lack of diversity of the alpha states (Stefan et al., 2018). The feature-selection strategy further underlined the importance of alpha activity for the classification of MCS vs. VS/UWS (Engemann et al., 2018; Sitt et al., 2014).

State transfer is essentially the sharing of Gaussian observation model bases. State segmentation is based on the likelihood estimation between the current observation and the Gaussian observation model bases and the probability of state transition. Thus, a possible limitation of the current method is the problem that the observed data could only be compulsorily attributed to one of the identified states. In the current study, we validated the state transfer results by measuring the normalized likelihood of the final segmented data with the Gaussian observation model bases. The state transfer showed outstanding reliability; the segmented data had a distinctly higher similarity with their corresponding model base (Fig. S7 in Supplementary Information) than with any of the other state descriptions. Otherwise, if the segmented data had close similarity with two or more Gaussian observation bases, they should be used with caution for this type of transfer analysis. Moreover, the state transfer process was tested first in the healthy subjects by a training and test split procedure, and by generation of surrogate data by random permutation of the time points (Fig. S6 in Supplementary Information). All

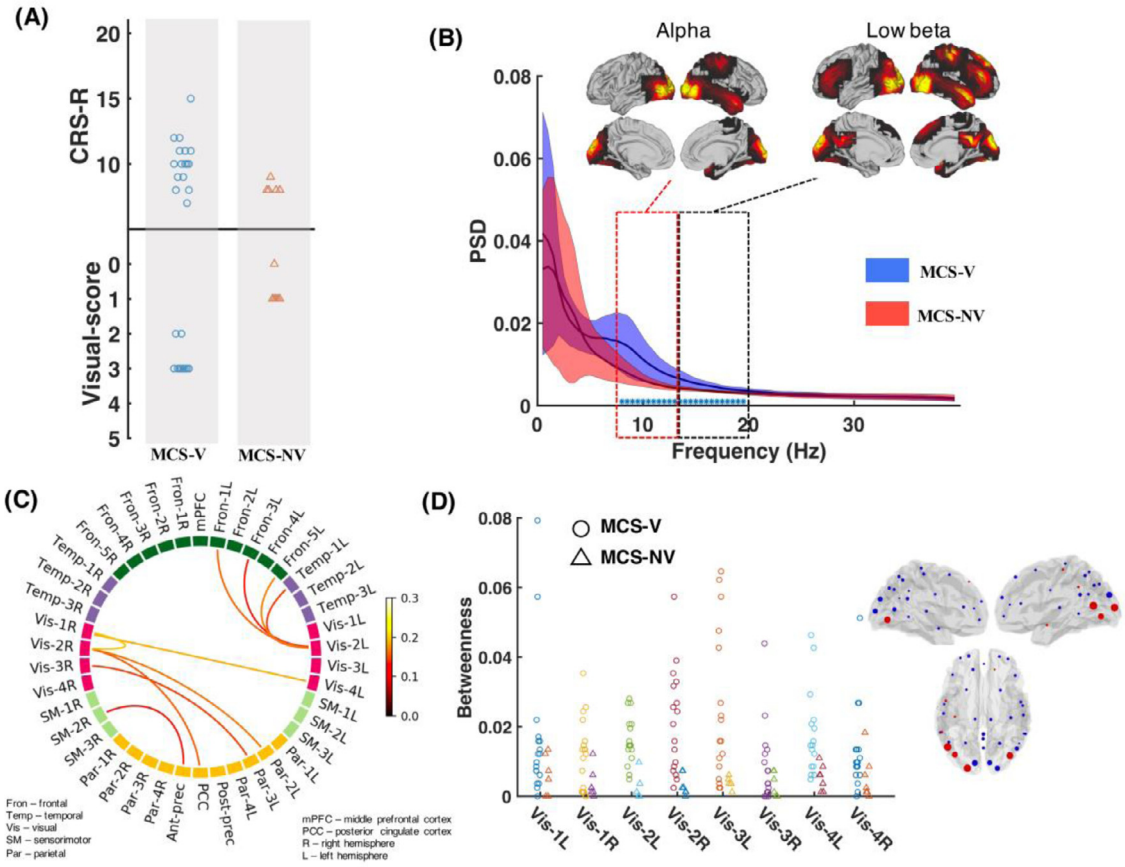


**Fig. 7.** Visual transient state in patients with a minimally conscious state (MCS). (A) Patients were classified into two groups according to the CRS-R visual behavioral assessment: presence of purposeful visual responses (MCS-V, CRS-R visual score > 1) or not (MCS-NV). (B) The PSD – frequency plot (mean ± 1SD; blue: MCS-V, red: MCS-NV) shows the frequency bins with group difference (* Kolmogorov–Smirnov tests with FDR correction, P < 0.05) at the visual regions during visual state expression. Patients with MCS-V exhibited higher alpha power in the bilateral visual regions (spatial plots) and higher low beta power in the right visual region compared with MCS-NV during visual state expression. (C) Lines in the connectivity plot representing the source space with 42 parcellations indicate significantly stronger connectivity (i.e., higher coherence values) in the alpha-low beta band of MCS-V vs. MCS-NV during the visual state expression. The color of the lines represents connectivity strength, as given in the color bar. (D) Hub values (betweenness) of the visual regions in MCS-V and MCS-NV. The visual regions played a significant hub role during visual state expression in MCS-V. The dot sizes represent the betweenness values, with the red ones indicating significantly higher hub values of MCS-V compared to MCS-NV (For interpretation of the references to color in this figure legend, the reader is referred to the web version of this article.).

validation measures consistently led to the firm conclusion that the four key transient states identified in the healthy subjects were also truly existing in the DOC patients (Fig. S5 in Supplementary Information), and were not artificially generated by the state transfer process.

The data quality is a critical factor in transient state analysis, regardless of state inference or transfer. For state inference, one or more Gaussian observation model bases would be needed to describe the features of an artefact in the case of low data quality. It would generate individually dominated meaningless states. For transfer analysis, the artefacts would also be compulsorily labeled as some states, which would affect the state features. The current study used a SOUND algorithm (Mutanen et al., 2018) to evaluate the data quality, which is based on the difference between the real channel signal and the ideal signal inferred by other channels based on a shared lead field. Thus, a high data quality represents a close relationship between different channels and is helpful for network description using a covariance matrix. However, compared with the MEG study that used 256 channels (Vidaurre et al., 2018b), the current EEG study was limited regarding signal quality and source space reconstruction, which could possibly explain the meaningless states that appeared in the analysis with K = 12. However, the four key transient states were robustly present in the data and had high similarity between inference with a different K number (Fig. S4 in Supplementary Information). Additionally, the stochastic estimation of HMM analysis pipeline added uncertainty in the state inference. A reproducibility test was conducted based on 30 repeated runs on the full data set. Although the results showed inconsistence of state expression to some extent, the group differences between healthy subjects and DOC patients were robustly present across the repeated runs (Fig. S12 in Supplementary Information).

EEG microstates analyses have been performed in DOC patients and revealed a relationship between lack of diversity and percentage of time spent in the alpha microstate with unconsciousness (Fingelkurts et al., 2012; Stefan et al., 2018). These findings could be partly interpreted from the results of the present study: suppression of alpha-dominated posterior and visual states in patients with DOC. Although both microstates and transient states identify short-lived brain states in the resting-state EEG, the underlying methodology of their analysis is completely different. Microstate analysis segments the EEG time series into predefined numbers of states according to clustering of topographies. It only takes sensor power distributions into account but does not consider the spectral and cross-spectral profiles like HMM does. In contrast, transient states are not only driven by spatial distribution of spectral power and phase-locking networks but also include temporal autocorrelation by taking into account historic state activation for the current state estimation. Therefore, the transient states interpret more detail and take into account more comprehensive properties from resting-state EEG than microstates do. Moreover, the transient states are estimated in source space, which suppresses the impact from noise and volume

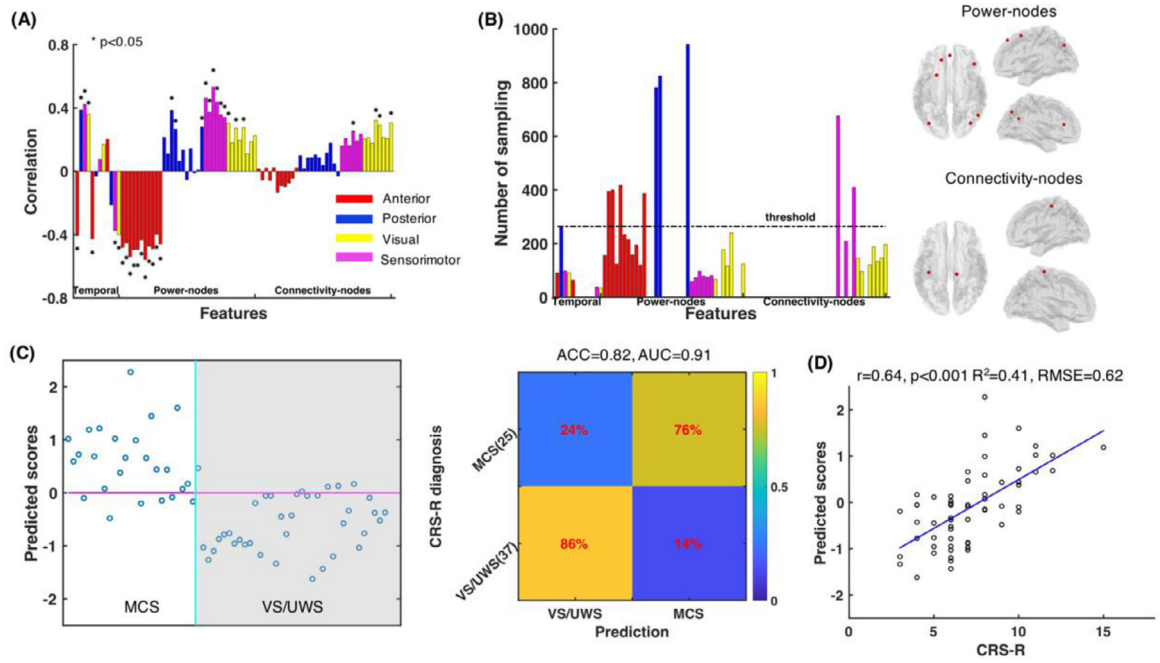


**Fig. 8.** Classification of patients with minimally conscious state (MCS) and vegetative state/unresponsive wakefulness syndrome (VS/UWS) using machine learning. (*A*) Pearson's correlation between the features and the CRS-R scores (*$P < 0.05$). (*B*) Number of appearance of transient state features, selected from the bootstrap sampling subsets. The selection strategy involved a couple of statistical tests and a competitive adaptive reweighted sampling method (for details, see Supplementary Information). The asterisks indicate significance in the statistical tests between MCS and VS/UWS ($P < 0.01$). The threshold was selected using a Gaussian mixture model. The features robustly appeared in the selection strategy included power nodes and connectivity nodes, which are displayed on top and lateral views of the brain at the right side. (*C*) Individually predicted scores for each patient with DOC using the nest machine learning structure. The pink line indicates the threshold for the binary classification. The right panel shows the classification accuracy of the patients with MCS vs. VS/UWS. ACC = accuracy of classification, AUC = area under the curve. (*D*) Scatter plot of the predicted scores and the CRS-R total scores of all DOC patients. $R^2$, coefficient of determination; RMSE, root mean squared error. (For interpretation of the references to color in this figure legend, the reader is referred to the web version of this article.)

conduction. Analysis of transient states enables us to draw significant relations between temporo-spatial brain activation and the patients' behavior and clinical status.

In conclusion, the current study provides a new perspective on the relationship between spontaneous transient states in brain networks and human consciousness. The transient states afford multidimensional information on the spontaneous activities, including spatial power patterns, temporal dynamics, spectral shifts, and connectivity construction, which cover most types of feature correlations with the alteration of consciousness. The transient states closely correlated with the consciousness level and conscious behaviors of patients with DOC. These findings will promote our understanding of the neurophysiological mechanisms underlying human consciousness.

## Data and code availability statement

The MATLAB scripts—including the EEG and MRI pre-processing pipeline, source construction and parcellation, transient state inference and transfer, and machine learning—are available at the https://github.com/BYJW/EEG-Transient-State. Related toolboxes can be accessed at https://github.com/OHBA-analysis and http://libpls.net/.

Original EEG datasets including healthy subjects and patients with DOC can be accessed with *link* (https://drive.google.com/drive/folders/1CFx1Q3RqZq5Vzig2tSUA1pFyloxBBuoB?usp=sharing).

Because of the privacy regulations of the collaborating hospital, the individual MR images can only be accessible by contacting Dr. Yi Yang (one of the authors, affiliation see above) with research application.

## Declaration of Competing Interest

The other authors declare that they have no conflicts of interest.

## Credit authorship contribution statement

**Yang Bai:** Visualization, Writing – original draft, Methodology, Formal analysis, Writing – review & editing. **Jianghong He:** Resources, Data curation, Writing – review & editing. **Xiaoyu Xia:** Resources, Data curation, Writing – review & editing. **Yong Wang:** Resources, Data curation, Writing – review & editing. **Yi Yang:** Resources, Data curation, Writing – review & editing. **Haibo Di:** Resources, Writing – review & editing. **Xiaoli Li:** Resources, Writing – review & editing. **Ulf Ziemann:** Visualization, Writing – original draft, Writing – review & editing.

## Acknowledgement

This work was supported by the National Natural Science Foundation of China (61901155); Medicine and Health Science and Technology Project of Zhejiang Province (2019RC254); and the Alexander-von-Humboldt foundation (3.5 - 1203399 - CHN - HFST-P).

## Supplementary materials

Supplementary material associated with this article can be found, in the online version, at doi:10.1016/j.neuroimage.2021.118407.

## References

Allen, E.A., Damaraju, E., Plis, S.M., Erhardt, E.B., Eichele, T., Calhoun, V.D., 2014. Tracking whole-brain connectivity dynamics in the resting state. Cereb. Cortex 24, 663–676.

Andersen, L.M., Pedersen, M.N., Sandberg, K., Overgaard, M., 2016. Occipital MEG activity in the early time range (<300 ms) predicts graded changes in perceptual consciousness. Cereb. Cortex 26, 2677–2688.

Baker, A.P., Brookes, M.J., Rezek, I.A., Smith, S.M., Behrens, T., Smith, Probert, P., J., Woolrich, M, 2014. Fast transient networks in spontaneous human brain activity. Elife 3, e01867.

Barttfeld, P., Uhrig, L., Sitt, J.D., Sigman, M., Jarraya, B., Dehaene, S., 2015. Signature of consciousness in the dynamics of resting-state brain activity. Proc. Natl. Acad. Sci. U S A 112, 887–892.
Bodien, Y.G., Chatelle, C., Edlow, B.L., 2017. Functional Networks in Disorders of Consciousness. Semin. Neurol. 37, 485–502.
Boly, M., Massimini, M., Tsuchiya, N., Postle, B.R., Koch, C., Tononi, G., 2017. Are the neural correlates of consciousness in the front or in the back of the cerebral cortex? Clinical and neuroimaging evidence. J. Neurosci. 37, 9603–9613.
Boly, M., Moran, R., Murphy, M., Boveroux, P., Bruno, M.A., Noirhomme, Q., Ledoux, D., Bonhomme, V., Brichant, J.F., Tononi, G., Laureys, S., Friston, K., 2012. Connectivity changes underlying spectral EEG changes during propofol-induced loss of consciousness. J. Neurosci. 32, 7082–7090.
Breshears, J.D., Roland, J.L., Sharma, M., Gaona, C.M., Freudenburg, Z.V., Tempelhoff, R., Avidan, M.S., Leuthardt, E.C., 2010. Stable and dynamic cortical electrophysiology of induction and emergence with propofol anesthesia. Proc. Natl. Acad. Sci. U S A 107, 21170–21175.
Bullmore, E., Sporns, O., 2009. Complex brain networks: graph theoretical analysis of structural and functional systems. Nat. Rev. Neurosci. 10, 186–198.
Bullmore, E., Sporns, O., 2012. The economy of brain network organization. Nat. Rev. Neurosci. 13, 336–349.
Buzsaki, G., 2006. Rhythms of the Brain. Oxford University Press.
Casali, A.G., Gosseries, O., Rosanova, M., Boly, M., Sarasso, S., Casali, K.R., Casarotto, S., Bruno, M.A., Laureys, S., Tononi, G., Massimini, M., 2013. A theoretically based index of consciousness independent of sensory processing and behavior. Sci. Transl. Med. 5 198-105.
Colclough, G.L., Woolrich, M.W., Tewarie, P., Brookes, M.J., Quinn, A.J., Smith, S.M., 2016. How reliable are MEG resting-state connectivity metrics? Neuroimage 138, 284–293.
Damaraju, E., Allen, E.A., Belger, A., Ford, J.M., Mcewen, S., Mathalon, D.H., Mueller, B.A., Pearlson, G.D., Potkin, S.G., Preda, A., Turner, J.A., Vaidya, J.G., Van Erp, T.G., Calhoun, V.D., 2014. Dynamic functional connectivity analysis reveals transient states of dysconnectivity in schizophrenia. Neuroimage Clin. 5, 298–308.
Damoiseaux, J.S., Rombouts, S.A., Barkhof, F., Scheltens, P., Stam, C.J., Smith, S.M., Beckmann, C.F., 2006. Consistent resting-state networks across healthy subjects. Proc. Natl. Acad. Sci. U S A 103, 13848–13853.
Deco, G., Jirsa, V.K., Mcintosh, A.R., 2011. Emerging concepts for the dynamical organization of resting-state activity in the brain. Nat. Rev. Neurosci. 12, 43–56.
Demertzi, A., Antonopoulos, G., Heine, L., Voss, H.U., Crone, J.S., De Los Angeles, C., Bahri, M.A., Di Perri, C., Vanhaudenhuyse, A., Charland-Verville, V., Kronbichler, M., Trinka, E., Phillips, C., Gomez, F., Tshibanda, L., Soddu, A., Schiff, N.D., Whitfield--Gabrieli, S., Laureys, S., 2015. Intrinsic functional connectivity differentiates minimally conscious from unresponsive patients. Brain 138, 2619–2631.
Demertzi, A., Gomez, F., Crone, J.S., Vanhaudenhuyse, A., Tshibanda, L., Noirhomme, Q., Thonnard, M., Charland-Verville, V., Kirsch, M., Laureys, S., 2014. Multiple fMRI system-level baseline connectivity is disrupted in patients with consciousness alterations. Cortex 52, 35–46.
Di, X., Gohel, S., Kim, E.H., Biswal, B.B., 2013. Task vs. rest—different network configurations between the coactivation and the resting-state brain networks. Front. Hum. Neurosci. 7, 493.
Engemann, D.A., Raimondo, F., King, J.R., Rohaut, B., Louppe, G., Faugeras, F., Annen, J., Cassol, H., Gosseries, O., Fernandez-Slezak, D., Laureys, S., Naccache, L., Dehaene, S., Sitt, J.D., 2018. Robust EEG-based cross-site and cross-protocol classification of states of consciousness. Brain 141, 3179–3192.
Ferrarelli, F., Massimini, M., Sarasso, S., Casali, A., Riedner, B.A., Angelini, G., Tononi, G., Pearce, R.A., 2010. Breakdown in cortical effective connectivity during midazolam-induced loss of consciousness. Proc. Natl. Acad. Sci. U S A 107, 2681–2686.
Fingelkurts, A.A., Fingelkurts, A.A., Bagnato, S., Boccagni, C., Galardi, G., 2012. EEG oscillatory states as neuro-phenomenology of consciousness as revealed from patients in vegetative and minimally conscious states. Conscious Cogn. 21, 149–169.
Fox, M.D., Snyder, A.Z., Vincent, J.L., Corbetta, M., Van Essen, D.C., Raichle, M.E., 2005. The human brain is intrinsically organized into dynamic, anticorrelated functional networks. Proc. Natl. Acad. Sci. U S A 102, 9673–9678.
Fransson, P., Marrelec, G., 2008. The precuneus/posterior cingulate cortex plays a pivotal role in the default mode network: Evidence from a partial correlation network analysis. Neuroimage 42, 1178–1184.
Giacino, J.T., Ashwal, S., Childs, N., Cranford, R., Jennett, B., Katz, D.I., Kelly, J.P., Rosenberg, J.H., Whyte, J., Zafonte, R.D., Zasler, N.D., 2002. The minimally conscious state: definition and diagnostic criteria. Neurology 58, 349–353.
Giacino, J.T., Kalmar, K., Whyte, J., 2004. The JFK Coma Recovery Scale-Revised: measurement characteristics and diagnostic utility. Arch. Phys. Med. Rehabil. 85, 2020–2029.
He, Y., Evans, A., 2010. Graph theoretical modeling of brain connectivity. Curr. Opin. Neurol. 23, 341–350.
Hillebrand, A., Barnes, G.R., 2005. Beamformer analysis of MEG data. Int. Rev. Neurobiol. 68, 149–171.
Huang, Z., Dai, R., Wu, X., Yang, Z., Liu, D., Hu, J., Gao, L., Tang, W., Mao, Y., Jin, Y., Wu, X., Liu, B., Zhang, Y., Lu, L., Laureys, S., Weng, X., Northoff, G., 2014. The self and its resting state in consciousness: an investigation of the vegetative state. Hum. Brain Mapp. 35, 1997–2008.
Hutchison, R.M., Womelsdorf, T., Allen, E.A., Bandettini, P.A., Calhoun, V.D., Corbetta, M., Della Penna, S., Duyn, J.H., Glover, G.H., Gonzalez-Castillo, J., Handwerker, D.A., Keilholz, S., Kiviniemi, V., Leopold, D.A., De Pasquale, F., Sporns, O., Walter, M., Chang, C., 2013. Dynamic functional connectivity: promise, issues, and interpretations. Neuroimage 80, 360–378.
Hyafil, A., Giraud, A.L., Fontolan, L., Gutkin, B., 2015. Neural Cross-Frequency Coupling: Connecting Architectures, Mechanisms, and Functions. Trends Neurosci. 38, 725–740.
Hyvarinen, A., Oja, E., 2000. Independent component analysis: algorithms and applications. Neural Netw. 13, 411–430.
Koch, C., 2018. What is consciousness? Nature 557, S8–S12.
Koch, C., Massimini, M., Boly, M., Tononi, G., 2016. Neural correlates of consciousness: progress and problems. Nat. Rev. Neurosci. 17, 307–321.
Laureys, S., Celesia, G.G., Cohadon, F., Lavrijsen, J., Leon-Carrion, J., Sannita, W.G., Sazbon, L., Schmutzhard, E., Von Wild, K.R., Zeman, A., Dolce, G.European Task Force on Disorders Of, C, 2010. Unresponsive wakefulness syndrome: a new name for the vegetative state or apallic syndrome. BMC Med. 8, 68.
Lee, U., Kim, S., Noh, G.J., Choi, B.M., Hwang, E., Mashour, G.A., 2009. The directionality and functional organization of frontoparietal connectivity during consciousness and anesthesia in humans. Conscious Cogn. 18, 1069–1078.
Lehembre, R., Bruno, M.A., Vanhaudenhuyse, A., Chatelle, C., Cologan, V., Leclercq, Y., Soddu, A., Macq, B., Laureys, S., Noirhomme, Q., 2012. Resting-state EEG study of comatose patients: a connectivity and frequency analysis to find differences between vegetative and minimally conscious states. Funct. Neurol. 27, 41–47.
Li, H.D., Xu, Q.S., Liang, Y.Z., 2018. libPLS: An integrated library for partial least squares regression and linear discriminant analysis. Chemom. Intell. Lab. Syst. 176, 34–43.
Martinez, D.E., Rudas, J., Demertzi, A., Charland-Verville, V., Soddu, A., Laureys, S., Gomez, F., 2020. Reconfiguration of large-scale functional connectivity in patients with disorders of consciousness. Brain Behav. 10, e1476.
Mcintosh, A.R., 2000. Towards a network theory of cognition. Neural Netw. 13, 861–870.
Mesulam, M.M., 1998. From sensation to cognition. Brain 121 (Pt 6), 1013–1052.
Mutanen, T.P., Metsomaa, J., Liljander, S., Ilmoniemi, R.J., 2018. Automatic and robust noise suppression in EEG and MEG: the SOUND algorithm. Neuroimage 166, 135–151.
Naro, A., Bramanti, A., Leo, A., Cacciola, A., Manuli, A., Bramanti, P., Calabro, R.S., 2018. Shedding new light on disorders of consciousness diagnosis: the dynamic functional connectivity. Cortex 103, 316–328.
Naro, A., Bramanti, P., Leo, A., Cacciola, A., Bramanti, A., Manuli, A., Calabro, R.S., 2016. Towards a method to differentiate chronic disorder of consciousness patients' awareness: the low-resolution brain electromagnetic tomography analysis. J. Neurol. Sci. 368, 178–183.
Odegaard, B., Knight, R.T., Lau, H., 2017. Should a few null findings falsify prefrontal theories of conscious perception? J. Neurosci. 37, 9593–9602.
Oostendorp, T.F., Van Oosterom, A., 1989. Source parameter estimation in inhomogeneous volume conductors of arbitrary shape. IEEE Trans. Biomed. Eng. 36, 382–391.
Piarulli, A., Bergamasco, M., Thibaut, A., Cologan, V., Gosseries, O., Laureys, S., 2016. EEG ultradian rhythmicity differences in disorders of consciousness during wakefulness. J. Neurol. 263, 1746–1760.
Power, J.D., Cohen, A.L., Nelson, S.M., Wig, G.S., Barnes, K.A., Church, J.A., Vogel, A.C., Laumann, T.O., Miezin, F.M., Schlaggar, B.L., Petersen, S.E., 2011. Functional network organization of the human brain. Neuron 72, 665–678.
Power, J.D., Fair, D.A., Schlaggar, B.L., Petersen, S.E., 2010. The development of human functional brain networks. Neuron 67, 735–748.
Qin, P., Wu, X., Huang, Z., Duncan, N.W., Tang, W., Wolff, A., Hu, J., Gao, L., Jin, Y., Wu, X., 2015. How are different neural networks related to consciousness? Ann. Neurol. 78, 594–605.
Quinn, A.J., Vidaurre, D., Abeysuriya, R., Becker, R., Nobre, A.C., Woolrich, M.W., 2018. Task-evoked dynamic network analysis through hidden markov modeling. Front. Neurosci. 12, 603.
Raichle, M.E., Macleod, A.M., Snyder, A.Z., Powers, W.J., Gusnard, D.A., Shulman, G.L., 2001. A default mode of brain function. Proc. Natl. Acad. Sci. U S A 98, 676–682.
Rosazza, C., Andronache, A., Sattin, D., Bruzzone, M.G., Marotta, G., Nigri, A., Ferraro, S., Rossi Sebastiano, D., Porcu, L., Bersano, A., Benti, R., Leonardi, M., D'incerti, L., Minati, L.Coma Research Center, B. I., 2016. Multimodal study of default-mode network integrity in disorders of consciousness. Ann. Neurol. 79, 841–853.
Rossi Sebastiano, D., Panzica, F., Visani, E., Rotondi, F., Scaioli, V., Leonardi, M., Sattin, D., D'incerti, L., Parati, E., Ferini Strambi, L., Franceschetti, S, 2015. Significance of multiple neurophysiological measures in patients with chronic disorders of consciousness. Clin. Neurophysiol. 126, 558–564.
Rubinov, M., Sporns, O., 2010. Complex network measures of brain connectivity: uses and interpretations. Neuroimage 52, 1059–1069.
Salvador, R., Suckling, J., Coleman, M.R., Pickard, J.D., Menon, D., Bullmore, E., 2005. Neurophysiological architecture of functional magnetic resonance images of human brain. Cereb. Cortex 15, 1332–1342.
Schiff, N.D., 2015. Cognitive motor dissociation following severe brain injuries. JAMA Neurol. 72, 1413–1415.
Selimbeyoglu, A., Parvizi, J., 2010. Electrical stimulation of the human brain: perceptual and behavioral phenomena reported in the old and new literature. Front. Hum. Neurosci. 4, 46.
Sitt, J.D., King, J.R., El Karoui, I., Rohaut, B., Faugeras, F., Gramfort, A., Cohen, L., Sigman, M., Dehaene, S., Naccache, L., 2014. Large scale screening of neural signatures of consciousness in patients in a vegetative or minimally conscious state. Brain 137, 2258–2270.
Soddu, A., Vanhaudenhuyse, A., Bahri, M.A., Bruno, M.A., Boly, M., Demertzi, A., Tshibanda, J.F., Phillips, C., Stanziano, M., Ovadia-Caro, S., Nir, Y., Maquet, P., Papa, M., Malach, R., Laureys, S., Noirhomme, Q., 2012. Identifying the default-mode component in spatial IC analyses of patients with disorders of consciousness. Hum. Brain Mapp. 33, 778–796.
Stefan, S., Schorr, B., Lopez-Rolon, A., Kolassa, I.T., Shock, J.P., Rosenfelder, M., Heck, S., Bender, A., 2018. Consciousness indexing and outcome prediction with resting-state EEG in severe disorders of consciousness. Brain Topogr. 31, 848–862.
Thul, A., Lechinger, J., Donis, J., Michitsch, G., Pichler, G., Kochs, E.F., Jordan, D., Ilg, R., Schabus, M., 2016. EEG entropy measures indicate decrease of cortical information processing in disorders of consciousness. Clin. Neurophysiol. 127, 1419–1427.

Tononi, G., Boly, M., Massimini, M., Koch, C., 2016. Integrated information theory: from consciousness to its physical substrate. Nat. Rev. Neurosci. 17, 450–461.
Van Den Heuvel, M.P., Hulshoff Pol, H.E., 2010. Exploring the brain network: a review on resting-state fMRI functional connectivity. Eur. Neuropsychopharmacol. 20, 519–534.
Vanhaudenhuyse, A., Noirhomme, Q., Tshibanda, L.J., Bruno, M.A., Boveroux, P., Schnakers, C., Soddu, A., Perlbarg, V., Ledoux, D., Brichant, J.F., Moonen, G., Maquet, P., Greicius, M.D., Laureys, S., Boly, M., 2010. Default network connectivity reflects the level of consciousness in non-communicative brain-damaged patients. Brain 133, 161–171.
Vidaurre, D., Abeysuriya, R., Becker, R., Quinn, A.J., Alfaro-Almagro, F., Smith, S.M., Woolrich, M.W., 2018a. Discovering dynamic brain networks from big data in rest and task. Neuroimage 180, 646–656.
Vidaurre, D., Hunt, L.T., Quinn, A.J., Hunt, B.a.E., Brookes, M.J., Nobre, A.C., Woolrich, M.W., 2018b. Spontaneous cortical activity transiently organises into frequency specific phase-coupling networks. Nat. Commun. 9, 2987.
Vidaurre, D., Quinn, A.J., Baker, A.P., Dupret, D., Tejero-Cantero, A., Woolrich, M.W., 2016. Spectrally resolved fast transient brain states in electrophysiological data. Neuroimage 126, 81–95.
Vidaurre, D., Smith, S.M., Woolrich, M.W., 2017. Brain network dynamics are hierarchically organized in time. Proc. Natl. Acad. Sci. U S A 114, 12827–12832.
Wu, X., Zou, Q., Hu, J., Tang, W., Mao, Y., Gao, L., Zhu, J., Jin, Y., Wu, X., Lu, L., Zhang, Y., Zhang, Y., Dai, Z., Gao, J.H., Weng, X., Zhou, L., Northoff, G., Giacino, J.T., He, Y., Yang, Y., 2015. Intrinsic functional connectivity patterns predict consciousness level and recovery outcome in acquired brain injury. J. Neurosci. 35, 12932–12946.
Yao, S., Song, J., Gao, L., Yan, Y., Huang, C., Ding, H., Huang, H., He, Y., Sun, R., Xu, G., 2015. Thalamocortical sensorimotor circuit damage associated with disorders of consciousness for diffuse axonal injury patients. J. Neurol. Sci. 356, 168–174.